SUSTAINABLE ENGINEERING

(eISSN:3083-8231)
Article
Volume 3, 2026
https://doi.org/10.51200/susten.v3i1.7515

Preparation, Characterisation, and Application of a Chitosan–Zeolite Adsorbent for Efficient Congo Red Dye Removal from Aqueous solutions

S M Anisuzzaman[1,2*], Wan Nur Rabiatul Adawiyah[2]

[1] Energy and Materials Research Group, Universiti Malaysia Sabah, UMS Road, 88400, Kota Kinabalu, Sabah, Malaysia.
[2] Chemical Engineering Program, Faculty of Engineering, Universiti Malaysia Sabah, UMS Road, 88400, Kota Kinabalu, Sabah, Malaysia.
*Correspondence: anis_zaman@ums.edu.my

*ORCID ID: 0000000165551768
Received: 27 March 2026, Accepted: 4 July 2026

Abstract: The presence of synthetic dyes such as Congo red (CR) in wastewater, particularly from the textile industries, poses serious threats to both the environment and human health. These dyes are not only toxic and potentially carcinogenic but are also chemically stable, making them difficult to break down using conventional treatment methods such as coagulation, oxidation, or biological processes. In this study, a chitosan–zeolite adsorbent (CZA) was developed and investigated for the removal of CR from aqueous solutions. The adsorbent was synthesised using a simple mixing method and thoroughly characterised using Fourier Transform Infrared Spectroscopy (FTIR), X-ray Diffraction (XRD), and Brunauer–Emmett–Teller (BET) surface area analysis. The results confirmed the successful formation of CZA, with relevant functional groups, a semi-crystalline structure, and a porous structure with a surface area of 34.01 m²/g. Batch adsorption experiments were conducted to study the influence of parameters such as pH, contact time, temperature, and adsorbent dosage on dye removal efficiency. The highest dye removal efficiency of 98.4% was achieved using 1.0 g of CZA under optimum conditions of a pH 2, a contact time of 120 min, and 25°C. The adsorption data were analysed using isotherm and kinetic models. Among the isotherm models evaluated, the Langmuir model provided the best fit (R^2 = 0.9980), indicating monolayer adsorption with a maximum adsorption capacity (q_{max}) of 89.29 mg/g. Kinetic modelling showed that the adsorption followed the pseudo-second-order model (R^2 = 0.9966), suggesting that chemisorption was the dominant mechanism. Overall, this study demonstrates that the CZA exhibits high adsorption efficiency and has considerable potential for application in the treatment of dye-contaminated wastewater.

Keywords: adsorption; chitosan-zeolite; Congo red; isotherm modelling; kinetics; wastewater treatment.

1. Introduction

The discharge of synthetic dyes from textile and allied industries has become a major environmental concern owing to their toxicity, potential carcinogenicity, and persistence in aquatic environments. Among these pollutants, Congo red (CR), an anionic azo dye, is extensively utilised because of its high aqueous stability and resistance to microbial

degradation [1,2]. The persistence of CR in water bodies deteriorates water quality and disrupts aquatic ecosystems by reducing light penetration and inhibiting photosynthetic activity [3]. Although various wastewater treatment technologies have been developed, the unique challenges associated with dye pollution remain difficult to address effectively [4]. Conventional chemical treatment methods, such as coagulation, flocculation, and oxidation, are widely employed; however, they may generate secondary pollutants requiring further treatment [5]. Furthermore, their relatively high operating costs limit their practical application, particularly in developing countries. Although biological treatment methods are more environmentally friendly, they are often ineffective in degrading complex dye molecules. Similarly, membrane filtration and advanced oxidation processes have demonstrated promising treatment performance; however, their high energy requirements and maintenance costs remain significant limitations. Among the available treatment technologies, adsorption has attracted considerable attention because of its simplicity, high removal efficiency, cost-effectiveness, and potential for adsorbent regeneration [6].

The choice of adsorbent significantly influences the performance of the adsorption process. Chitosan, a biopolymer derived from chitin, possesses desirable properties including biodegradability, biocompatibility, and the presence of functional groups (–NH_2 and –OH) that interact with dye molecules [7-9]. Zeolite, on the other hand, is a naturally occurring aluminosilicate with high porosity, thermal stability, and ion-exchange capacity [8]. In addition, chitosan is biodegradable, non-toxic, and readily available, making it an attractive material for wastewater treatment applications. However, both materials have inherent limitations when used individually; chitosan exhibits relatively poor mechanical strength, whereas zeolite possesses fewer reactive functional groups for dye binding. To overcome these limitations, a hybrid chitosan–zeolite adsorbent (CZA) was developed. Although chitosan and zeolite have been individually investigated for dye adsorptions, studies on their combined use as a composite adsorbent for Congo red removal remain limited. The combination of these two materials is expected to enhance adsorption performance by integrating the favourable properties of each component. Fan et al. [4] reported that incorporating natural zeolite into chitosan enhanced the adsorption capacity for pollutant removal. The composite integrates the advantages of both materials, providing a porous, stable structure with abundant active sites for dye binding. The combination of the high surface area and ion-exchange capacity of zeolite with the functional versatility and biodegradability of chitosan makes the composite a promising adsorbent for dye removal from aqueous solutions [10]. Zeolite is characterized by its highly porous structure composed of a great surface area, thus the number of active sites available to capture the dye molecules will increase significantly. This property, when provided to chitosan, enables it to capture more dye molecules than chitosan combined with materials not endowed with a porous structure.

Despite the increasing interest in chitosan- and zeolite-based adsorbents, comprehensive studies on chitosan–zeolite composite adsorbents for Congo red removal, particularly those involving adsorption mechanism analysis through isotherm and kinetic modelling, remain limited. Therefore, this study aimed to synthesise, characterise, and evaluate a chitosan–zeolite adsorbent for the removal of Congo red from aqueous solutions. The adsorbent was characterised using Fourier Transform Infrared Spectroscopy (FTIR), X-ray Diffraction (XRD), and Brunauer–Emmett–Teller (BET) analysis, while its adsorption performance was

evaluated through batch adsorption experiments under different operating conditions, including pH, contact time, temperature, and adsorbent dosage. Furthermore, adsorption isotherm and kinetic models were employed to elucidate the adsorption mechanism and evaluate the adsorption performance of the developed composite.

2. Materials and methods

2.1. Materials and Chemicals

Zeolite A and chitosan were purchased from Sigma-Aldrich. Congo red (CR) dye, the target pollutant in this study, was also purchased from Sigma-Aldrich. Additional chemicals included 2% acetic acid for dissolving chitosan, 2 M sodium hydroxide (NaOH) for pH adjustment, hydrochloric acid (HCl), and deionised water for preparing solutions and adjusting the pH. The equipment used in this study included a magnetic stirrer for mixing, an analytical balance (Mettler Toledo) for measuring sample mass, an oven for drying the adsorbent, a pH meter for pH monitoring and adjustment, a JASCO UV–Vis spectrophotometer for concentration measurements, and a centrifuge for phase separation.

2.2. Preparation of Chitosan–Zeolite Adsorbent (CZA)

The chitosan–zeolite adsorbent (CZA) was synthesised by adapting the method reported by Şanlı & Demirhan [11], in which the chitosan-to-zeolite ratio was retained, while the quantities of the materials were adjusted to suit the present experimental setup. First, 6 g of chitosan was dissolved in 300 mL of a 2% acetic acid under continuous stirring using a magnetic stirrer. Simultaneously, 30 g of zeolite was dispersed in 300 mL of distilled water and stirred for 30 min to create a uniform suspension. The zeolite suspension was then slowly added to the chitosan solution over a period of 1.5 h under continuous stirring at 300 rpm to ensure homogeneous mixing. The pH of the resulting mixture was adjusted to 9 by the dropwise addition of 2 M NaOH while being monitored using a calibrated pH meter. This pH adjustment induced precipitation of the adsorbent. The precipitate was washed repeatedly with distilled water until the wash water reached approximately pH 7, ensuring the removal of residual chemicals. Finally, the adsorbent was dried in an oven at 105°C for 24 h, or until a constant mass was achieved, yielding a stable CZA for subsequent characterisation and adsorption studies.

2.3. Preparation of CR Dye Solution

A 1000 ppm stock solution of CR dye was prepared by dissolving 1 g of the dye in 1 L of distilled water. The stock solution was subsequently diluted to prepare working solutions with concentrations of 1, 5, 10, 15, and 20 ppm. These working solutions were used in the batch adsorption experiments to evaluate the adsorption capacity and efficiency of the synthesised adsorbent.

2.4. Characterisation of Adsorbent

Several analytical techniques were employed to characterise the physicochemical properties of the CZA to investigate its structure, chemical composition, and adsorption potential. Fourier Transform Infrared Spectroscopy (FTIR) was used to identify the functional groups present in

the composite and to evaluate the chemical interactions between chitosan and zeolite, which are responsible for its adsorption properties. A 2 g sample of the composite was mixed with potassium bromide (KBr) and pressed into a transparent pellet for FTIR analysis. The prepared pellet was then placed in the infrared beam path of a Bruker Vertex 70 FTIR spectrometer equipped with a D-LaTGS detector for spectral analysis.

X-ray Diffraction (XRD) analysis was performed to determine the crystalline structure of the adsorbent and to evaluate the degree of zeolite incorporation within the chitosan matrix. The XRD patterns also provided information on the phase composition and crystallinity of the composite. The analysis was carried out using a Bruker D2 Phaser diffractometer over a 2θ range of 5°–45°, equipped with a LynxEye detector (192 channels) and Cu (= 1.54 Å). Slit = 0.6 nm, ACS = 1, detector = 5.82 keV, duration time = 0.1 s, step size = 0.02° were the analysis parameters.

The Brunauer–Emmett–Teller (BET) method was used to determine the specific surface area and pore characteristics of the adsorbent, which are important parameters for evaluating its adsorption performance. Nitrogen adsorption–desorption isotherms at 77 K were measured using an ASAP 2420 surface area analyser (Micromeritics, USA) to determine the specific surface area (SBET), desorption pore volume at the relative pressure (P/PO), and average pore diameter. Approximately 1 g of the CZA composite was weighed for BET analysis.

2.5. Batch Adsorption Experiments

The adsorption efficiency of the CZA towards CR dye was systematically evaluated under different operational conditions to determine the optimum adsorption performance. The effects of four operational parameters, namely pH, contact time, temperature, and adsorbent dosage, were investigated. All experiments were conducted in triplicate, and the average values were plotted graphically.

To investigate the effect of pH, 100 mL of a 20 mg/L CR dye solution was adjusted to pH values of 2, 4, 5, 7, 9, and 10 using 0.1 M HCl or 0.1 M NaOH. Each solution was treated with 0.5 g of CZA and stirred at 500 rpm for 60 min at 25 ± 1°C. The selected pH range was adopted based on the study reported by Şanlı and Demirhan [11] on chitosan-based adsorbents.

To evaluate the effect of contact time, 100 mL of a 20 mg/L CR solution at the optimum pH (pH 2) was treated with 0.5 g of CZA and stirred at 200 rpm. Samples were collected at 10, 30, 60, 90, 120, 140, and 160 min for analysis.

The effect of temperature was investigated at 25, 35, 45 and 55°C using a fixed CR concentration of 20 mg/L, an adsorbent dosage of 0.5 g, and the optimum contact time of 120 min, as determined from the contact time study.

The effect of adsorbent dosage was evaluated by varying the amount of CZA from 0.1 to 1.0 g in 100 mL of a 20 mg/L CR solution under the optimum pH and contact time conditions.

2.6. Adsorption Data Analysis

The adsorption data were analysed by first constructing a standard calibration curve for CR. The calibration curve was prepared using CR solutions with concentrations of 1, 5, 10, 15, and 20 mg/L. The absorbance of each standard solution was measured at 497 nm, corresponding to the maximum absorption wavelength (λmax) of CR, using a UV–Visible spectrophotometer [12]. The absorbance of the experimental samples was then measured and compared with the standard calibration curve to determine the remaining dye concentration. The adsorption capacity (Q_e) was calculated using the Equation (1):

$$Q_e = \frac{(C_o - C_e)V}{m} \quad (1)$$

where C_o represents the initial dye concentration (mg/L), C_e represents the dye concentration at equilibrium (mg/L), V represents the volume of dye solution (L) and m represents the mass of adsorbent (g). The dye removal efficiency was calculated using Equation (2) [11]:

$$Removal\ efficiency\ \% = \frac{C_o - C_e}{C_o} \times 100 \quad (2)$$

where C_o represents the initial dye concentration (mg/L) and C_e represents the dye concentration at equilibrium (mg/L).

(a) Adsorption Isotherm Models

The Langmuir isotherm is expressed in its linear form as Equation (3):

$$\frac{C_e}{Q_e} = \frac{C_e}{q_{max}} + \frac{1}{K_L q_{max}} \quad (3)$$

where, Q_e is the amount of adsorbate adsorbed at equilibrium (mg/g), q_{max} is the maximum adsorption capacity (mg/g), K_L is the Langmuir constant (L/mg), C_e is the equilibrium concentration of adsorbate (mg/L).

By plotting $\frac{C_e}{Q_e}$ against C_e, the slope and intercept of the linear graph yield $\frac{1}{q_{max}}$ and $\frac{1}{K_L q_{max}}$ respectively. This plot assists in calculating the Langmuir constant K_L and the maximum adsorption capacity q_{max}, which are indicative of the potential of the CZA composite's surface area and pore properties. The dimensionless separation factor or equilibrium parameter, R_L, is calculated using Equation (4):

$$R_L = \frac{1}{K_L C_o} \quad (4)$$

where, C_o is the initial concentration of the adsorbate (mg/L.

The mathematical expression for the linear form of the Freundlich isotherm is expressed as Equation (5):

$$logQ_e = \frac{1}{n} logC_e + logK_F \quad (5)$$

where C_e is the equilibrium concentration of adsorbate (mg/L), Q_e is the amount of adsorbate adsorbed at equilibrium (mg/g). n is a dimensionless constant indicating the adsorption intensity, while K_F is the Freundlich constant, which indicates the adsorption capacity.
The Temkin isotherm is typically represented as Equation (6):

$$Q_e = \frac{RT}{b_T}\ln A_T + \frac{RT}{b_T}\ln C_e \quad (6)$$

where C_e is the equilibrium concentration of adsorbate (mg/L), b_T is the Temkin constant (J/mol), which accounts for the heat of adsorption, A_T is the Temkin isotherm constant at equilibrium, which displays the binding strength, R is the universal gas constant, T is the temperature, Q_e is the amount of adsorbate adsorbed at equilibrium (mg/g).

(b) Adsorption Kinetics Models

The fundamental expression of the Pseudo-first order (PFO) model is expressed as Equation (7):

$$\frac{dQ_t}{d_t} = k_1(Q_e - Q_t) \quad (7)$$

After integration, the linear form of the PFO model is given by Equation (8):

$$ln(Q_e - Q_t) = -k_1 t + lnQ_e \quad (8)$$

where, Q_t is the amount of adsorbate at time t (mg/g), k_1 is the rate constant for the PFO reaction (1/min), t represents the time, and Q_e is the amount of adsorbate at equilibrium (mg/g).

The Pseudo-second order (PSO) model is expressed as Equation (9):

$$\frac{dQ_t}{d_t} = k_2(Q_e - Q_t)^2 \quad (9)$$

where, Q_t is the amount of adsorbate adsorbed at time t (mg/g, Q_e is the amount of adsorbate at equilibrium (mg/g), and k_2 is the rate constant for the PSO reaction (g/mg·min).

After integration, the arranged linear form of the PSO equation is expressed as Equation 10:

$$\frac{t}{Q_t} = \frac{1}{k_2 Q_e^2} + \frac{t}{Q_e} \quad (10)$$

The pseudo-second-order rate constant (k_2) was determined from the slope of the linear plot, whereas the equilibrium adsorption capacity (Q_e) was determined from the intercept.

3. Results and Discussion

3.1. Characterisation of Chitosan–Zeolite Adsorbent (CZA)

3.1.1. FTIR Analysis

The FTIR analysis of the chitosan–zeolite adsorbent (CZA) was carried out to identify the functional groups present on the surface of the adsorbent. The FTIR spectrum is presented in Figure 1, which exhibits prominent absorption peaks at 976.07, 547.11, and 462.17 cm^{-1}. These

absorption bands correspond to characteristic vibrational modes that reflect the chemical structure and functional groups of the composite adsorbent.

A strong absorption band observed at approximately 976.07 cm^{-1} is attributed to C–O stretching vibrations. This band falls within the fingerprint region (1200–850 cm^{-1}), which is characteristic of carbohydrate and polysaccharide structures, where C–O and C–C bond vibrations together with ring deformation are commonly observed [13]. The absorption band may also be attributed to the asymmetric stretching vibrations of Si–O–Si or Si–O–Al bonds within the zeolite framework, confirming the successful incorporation of both chitosan and zeolite into the composite. Furthermore, these functional groups provide potential active sites for the adsorption of Congo red dye through hydrogen bonding and electrostatic interactions.

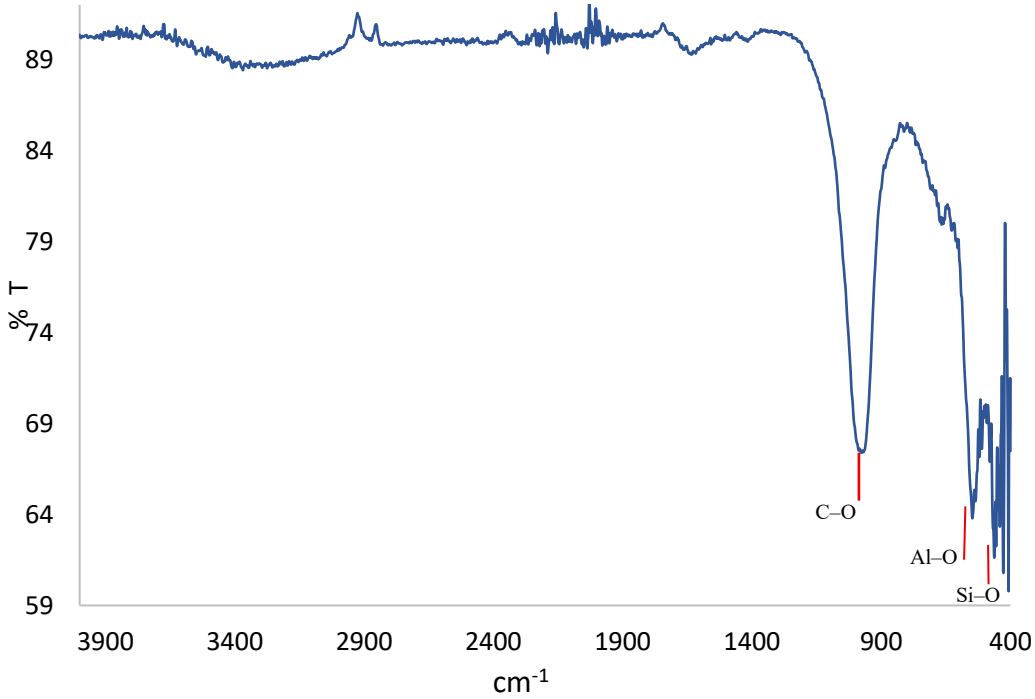

Figure 1. FTIR analysis of CZA

The absorption bands observed at approximately 461–462 cm^{-1} and 541 cm^{-1} are characteristic of internal bending vibrations within zeolite's tetrahedral framework, attributed to Si–O and Al–O bonds in the T–O–T structures (T = Si or Al), and are widely reported as signature bands in FTIR spectra of zeolites [14,15]. Their presence indicates that the aluminosilicate units remained intact after composite preparation, demonstrating that the crystalline structure of the zeolite was preserved during synthesis. The presence of several clear peaks in this area suggests a strong and stable zeolite structure, which helps improve the adsorbent's ability to adsorb dyes.

3.1.2. XRD Analysis

The XRD analysis was performed to investigate the crystal structure and purity of the synthesised CZA [16]. The diffractogram presented in Figure 2 exhibits several sharp and strong peaks within the 2θ range between 7° and 35°. These peaks correspond well with the

characteristic crystal structure of zeolite, suggesting that the zeolite's crystal structure was retained following composite synthesis.

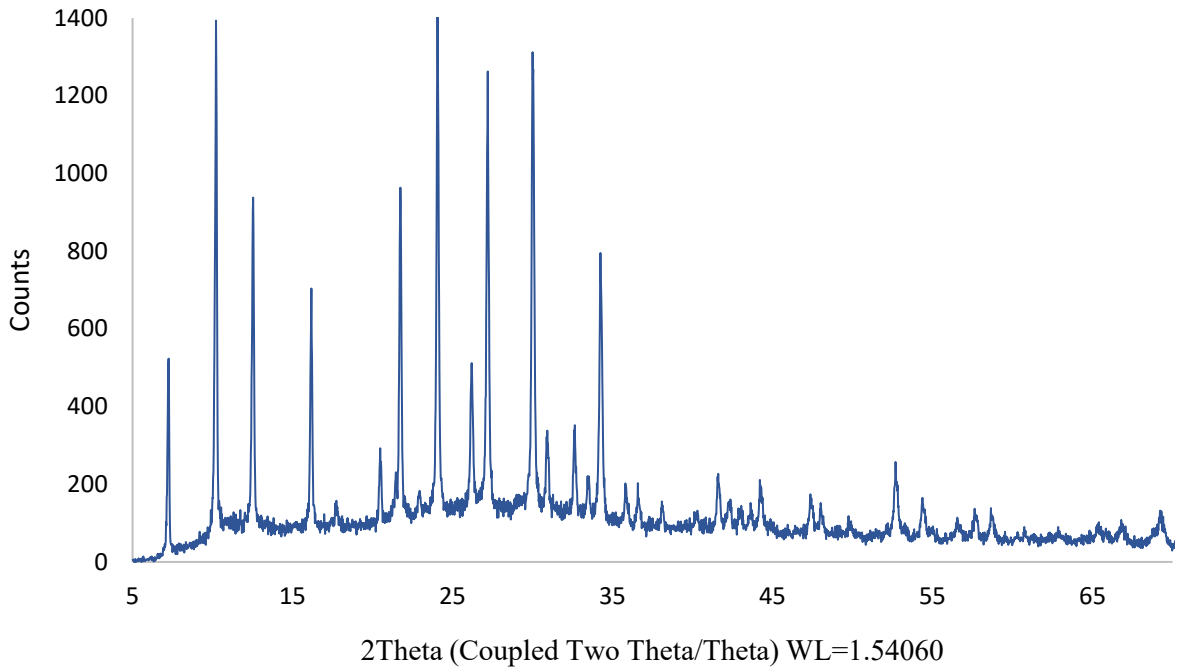

Figure 2. XRD pattern of CZA

The main peaks at around 2θ = 7.2°, 10.2°, 12.4°, 16.1°, 21.6°, 24.0°, 27.1°, and 30.0° are in good agreement with those reported for zeolite A in previous studies [17]. The sharp and intense peaks indicate that the zeolite retained a high degree of crystallinity even after being incorporated into the chitosan matrix to form the composite. On the other hand, the broad hump observed between 2θ = 15° and 30° is attributed to the amorphous nature of chitosan. As chitosan lacks long-range molecular order, it typically appears as a broad, low-intensity background signal in the XRD pattern. Overall, the XRD data demonstrate that the two materials were successfully combined to form a composite with favourable structural characteristics for adsorption. These findings are also consistent with those reported by Şanlı & Demirhan [11], who observed similar diffraction patterns in their chitosan composites for dye removal.

3.1.3. BET Analysis

The BET analysis was carried out to determine the surface area, pore volume, and pore size distribution of the synthesised CZA. The analysis was conducted at 77 K using nitrogen gas as the adsorbate. The results provide important information on the texture and surface features of the adsorbent, which are essential for evaluating its suitability for dye removal, particularly for large anionic dyes such as Congo red (CR). The nitrogen adsorption–desorption isotherm of CZA is presented in Figure 3.

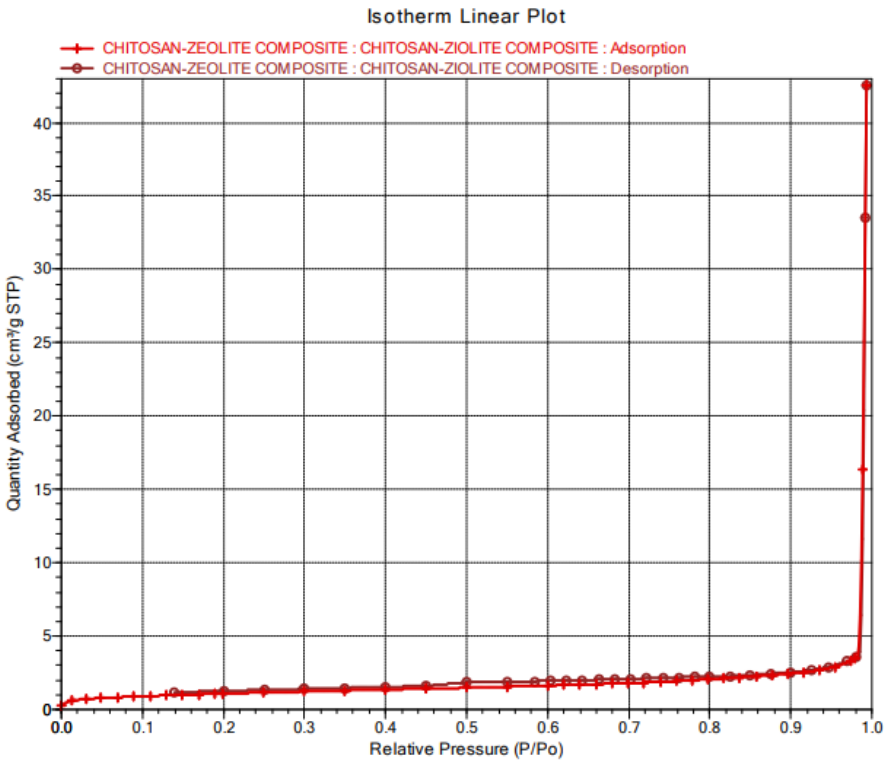

Figure 3. Nitrogen adsorption–desorption isotherm of CZA at 77 K

The curve follows a Type IV isotherm with an H3 hysteresis loop, based on IUPAC classification. This type of isotherm is characteristic of mesoporous materials and indicates the occurrence of capillary condensation within the pores at relatively high pressures (P/Po > 0.8). The H3 loop also suggests that the pores are slit-shaped or formed between plate-like particles, which is common in materials like zeolite flakes combined with polymers like chitosan. This shows that the adsorbent has a good mesoporous structure, which is useful for adsorbing larger organic molecules. The sharp increase in adsorption volume at higher P/Po values further supports the presence of wider mesopores and capillary condensation behaviour. The BET surface area was measured to be 34.01 m^2/g, indicating a moderately large surface area that contributes to dye adsorption [18]. The pore size distribution was determined using the Barrett–Joyner–Halenda (BJH) method, based on the desorption branch of the isotherm. The result shows a main pore diameter of approximately 952.21 Å, indicating that the material is predominantly macroporous (mesopores range from 20 to 500 Å or 2–50 nm). The total pore volume (at P/Po = 0.9) is 0.00394 cm^3/g, the average pore diameter (BJH Desorption) is 952.21 Å, and the cumulative pore area (BJH) is around 2.7 m^2/g. The large pore size and moderate pore volume suggest that dye molecules can easily diffuse into the pores, even though the overall surface area is relatively low.

3.2. Effects of Process Parameters on the Removal of Congo Red (CR)

3.2.1. Effect of pH

The effect of pH on the adsorption efficiency of CR dye using CZA is shown in Figure 4. The experimental data demonstrate a significant influence of pH on dye removal efficiency, where adsorption performance is notably enhanced under acidic conditions and diminished in basic environments [19,20]. At pH 2, the adsorption efficiency reached its highest value of 82.44%,

indicating that acidic conditions favour the adsorption process. As the pH increased from 2 to 10, a sharp decline in removal efficiency was observed, with the lowest efficiency of 18.78% recorded at pH 10.

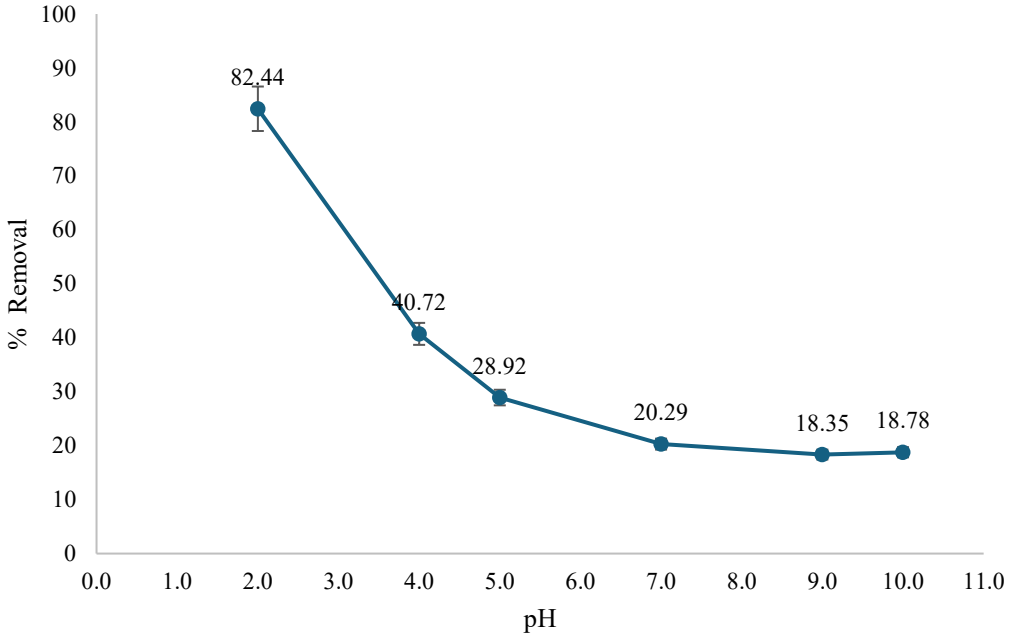

Figure 4. Effect of pH on CR dye removal by CZA

In an acidic environment, the surface of the adsorbent becomes more positively charged, thereby increasing the electrostatic attraction between the positively charged adsorbent and the negatively charged CR dye anions. This mechanism is consistent with previous studies on dye adsorption, including those by Ali et al. [21] and Dutta et al. [22], which reported enhanced dye removal under low pH conditions due to stronger coulombic interactions. Moreover, the dye molecules themselves can experience changes in ionisation state at different pH values, further affecting their interaction with the adsorbent [23]. Additionally, the structural characteristics of CR, which is an anionic diazo dye, make it more susceptible to electrostatic influences [24]. At high pH levels, reduced hydrogen bonding and van der Waals interactions between the dye and the adsorbent may also contribute to the lower adsorption performance. From a practical perspective, these findings highlight the importance of pH control in wastewater treatment processes involving CR dye and CZA. Operating under acidic conditions, particularly around pH 2, significantly enhances the dye removal efficiency [25].

3.2.2 Effect of Contact Time

The influence of contact time on the adsorption of CR dye by the CZA is presented in Figure 5. The results indicate that contact time is a critical factor in achieving efficient dye removal [18,26]. As contact time increased from 10 to 120 min, the percentage removal of CR significantly improved, reaching a maximum efficiency of 86.26% at 120 min.

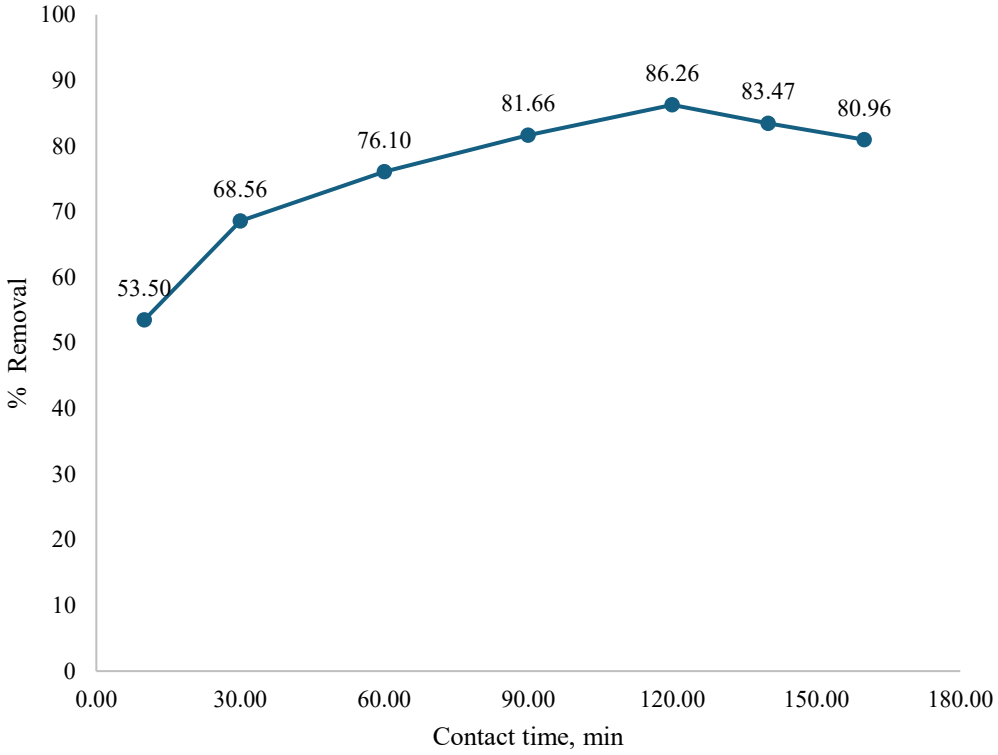

Figure 5. Effect of contact time on CR dye removal by CZA

In the early stage of adsorption, the process is primarily driven by the external surface interaction between the dye molecules and the adsorbent. This is evident from the initial removal percentage of 53.50% at 10 min, indicating that more than half of the dye was rapidly adsorbed [25]. Between 30 and 120 min, the rate of dye removal begins to slow down as many of the active sites become occupied. The reduced removal rate during this phase can be attributed to increased resistance to mass transfer, diffusion limitations, and possible pore blockage as the dye molecules move deeper into the internal structure of the adsorbent [27]. At 120 minutes, the adsorption reached equilibrium, at which the maximum dye uptake was achieved under the experimental conditions. However, beyond this point (140 min), a slight reduction in removal efficiency was observed, decreasing to 83.47%. This reduction may be attributed to several factors. First, desorption of weakly bound dye molecules can occur over prolonged contact times, particularly when adsorption is governed by weaker van der Waals interactions or physical adsorption [27,28]. Second, surface restructuring or pore blockage may occur after extended agitation, altering the physical accessibility of adsorption sites and reducing further uptake. Another possible explanation is the redistribution of adsorbed molecules at the adsorbent surface, resulting in minor disturbances in equilibrium and possibly resulting in desorption. This is particularly relevant in composite materials like CZA, where the polymer matrix may swell slightly or shift under mechanical stirring, impacting the availability and retention of active sites [28]. These results suggest that 120 min is the optimum contact time for achieving maximum adsorption efficiency for CR using the CZA. The optimum contact time ensures efficient utilisation of the adsorbent's active sites while achieving high removal efficiency of CR from aqueous solutions [29].

3.2.3. Effect of Temperature

The results presented in Figure 6 demonstrate that temperature has a significant effect on the adsorption efficiency of CR dye using CZA. The highest removal efficiency of 84.0% was recorded at 25°C. As the temperature increased to 35°C and 45°C, the removal efficiency decreased to 76.4% and 70.2%, respectively. At a further increase to 55°C, the removal efficiency was predicted to decrease to approximately 66%, indicating a continued downward trend with increasing temperature [15].

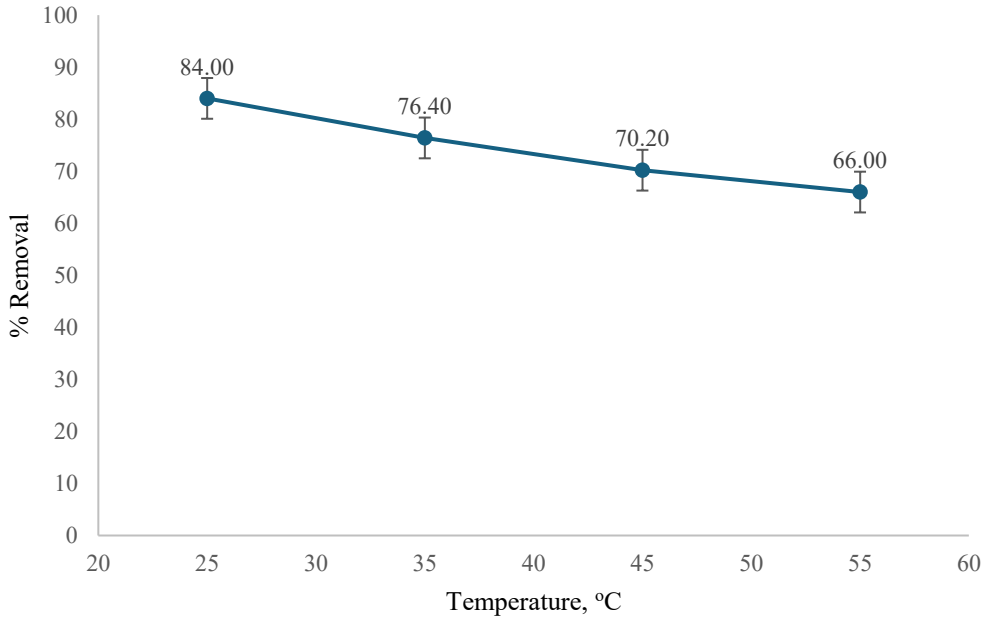

Figure 6. Effect of temperature on CR dye removal by CZA

These results suggest that the adsorption process is more effective at lower temperatures. At higher temperatures, dye molecules gain more kinetic energy and move more actively, thereby reducing their probability of being adsorbed onto the adsorbent surface [30]. Furthermore, higher temperatures may induce structural changes in the adsorbent. In some cases, the surface of the CZA might change slightly, affecting the availability of active sites. The chitosan component, for example, can swell or shrink, which might block some of the pores or reduce the surface area available for dye molecules to interact with [28,31]. Consequently, the overall adsorption capacity and removal efficiency decrease. From a practical perspective, these findings suggest that operating the adsorption process at lower temperatures is advantageous. This not only improves the dye removal efficiency but also reduces energy consumption by eliminating the need to heat the system [32].

3.2.4. Effect of Adsorbent Dosage

The results presented in Figure 7 demonstrate that the adsorbent dosage has a significant affect the efficiency of CR dye removal. As the adsorbent dosage increased from 0.1 g to 1 g, the removal efficiency increased drastically from 50% to 98.4% [29]. At the same time, the adsorption capacity decreased from 10 mg/g to 1.97 mg/g. This substantial improvement in removal efficiency can be attributed to the greater number of available adsorption sites provided by the higher adsorbent dosage. At lower dosages, there are not enough sites, so many

dye molecules remain in the solution, leading to lower removal percentages. As the dosage increases, there is more surface area and more active sites, which allow almost all the dye molecules to be adsorbed [28]. The highest dye removal efficiency of 98.4% was achieved using 1.0 g of the CZA under the optimum operating conditions, namely pH 2, a contact time of 120 min, and a temperature of 25°C. The increased adsorbent dosage provided a greater surface area and more active sites, allowing enhanced interaction between the dye molecules and the adsorbent. These findings indicate that 1.0 g is the optimum adsorbent dosage under the experimental conditions investigated.

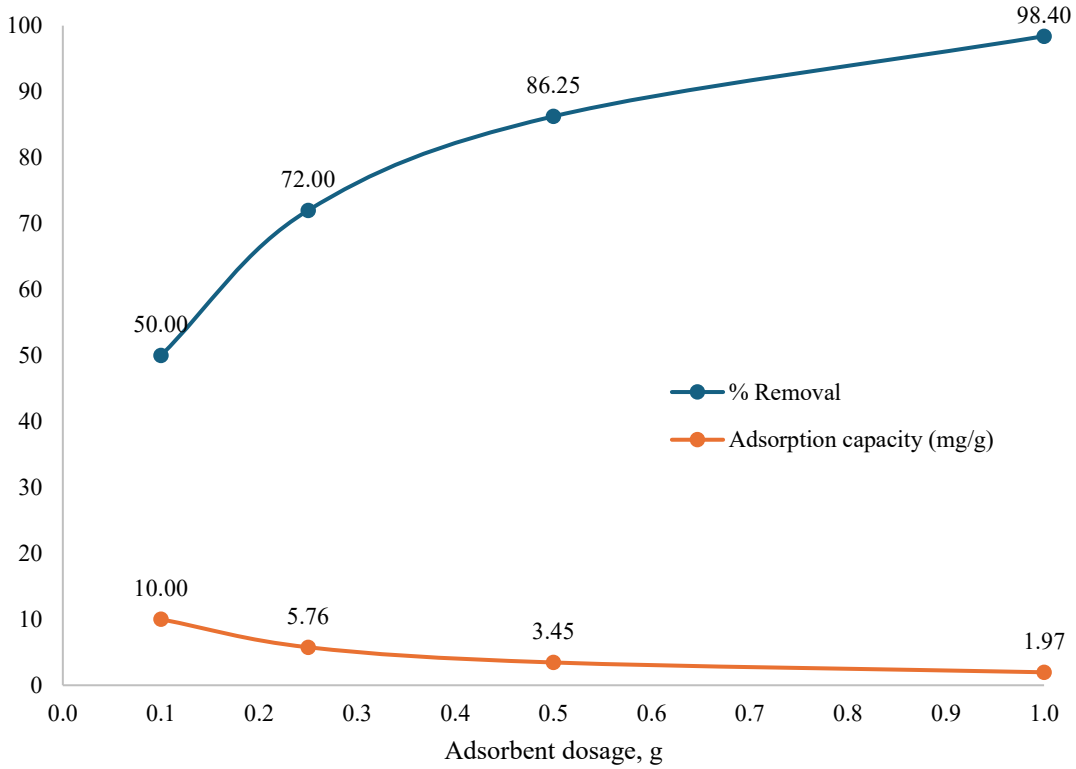

Figure 7. Effect of adsorbent dosage on CR dye removal and adsorbent capacity

Although increasing the adsorbent dosage significantly enhanced the removal efficiency of CR, excessive adsorbent usage may increase operational costs and generate additional spent adsorbent requiring handling or disposal [33]. Therefore, an optimum adsorbent dosage should be selected to balance adsorption performance, operational cost, and the sustainability of the wastewater treatment process [34].

3.3. Adsorption Isotherm Analysis

Based on the plots shown in Figure 8(a–c), the Langmuir isotherm model exhibited the highest coefficient of determination (R^2 = 0.9980), indicating that it provided the best fit to the experimental adsorption data for CR on CZA. This suggests that the adsorption process occurs predominantly as monolayer adsorption on the surface of CZA, where the active sites are assumed to be homogeneous and equally accessible to the dye molecules. According to the Langmuir model, once a dye molecule occupies an adsorption site, no further adsorption can occur at that site [35].

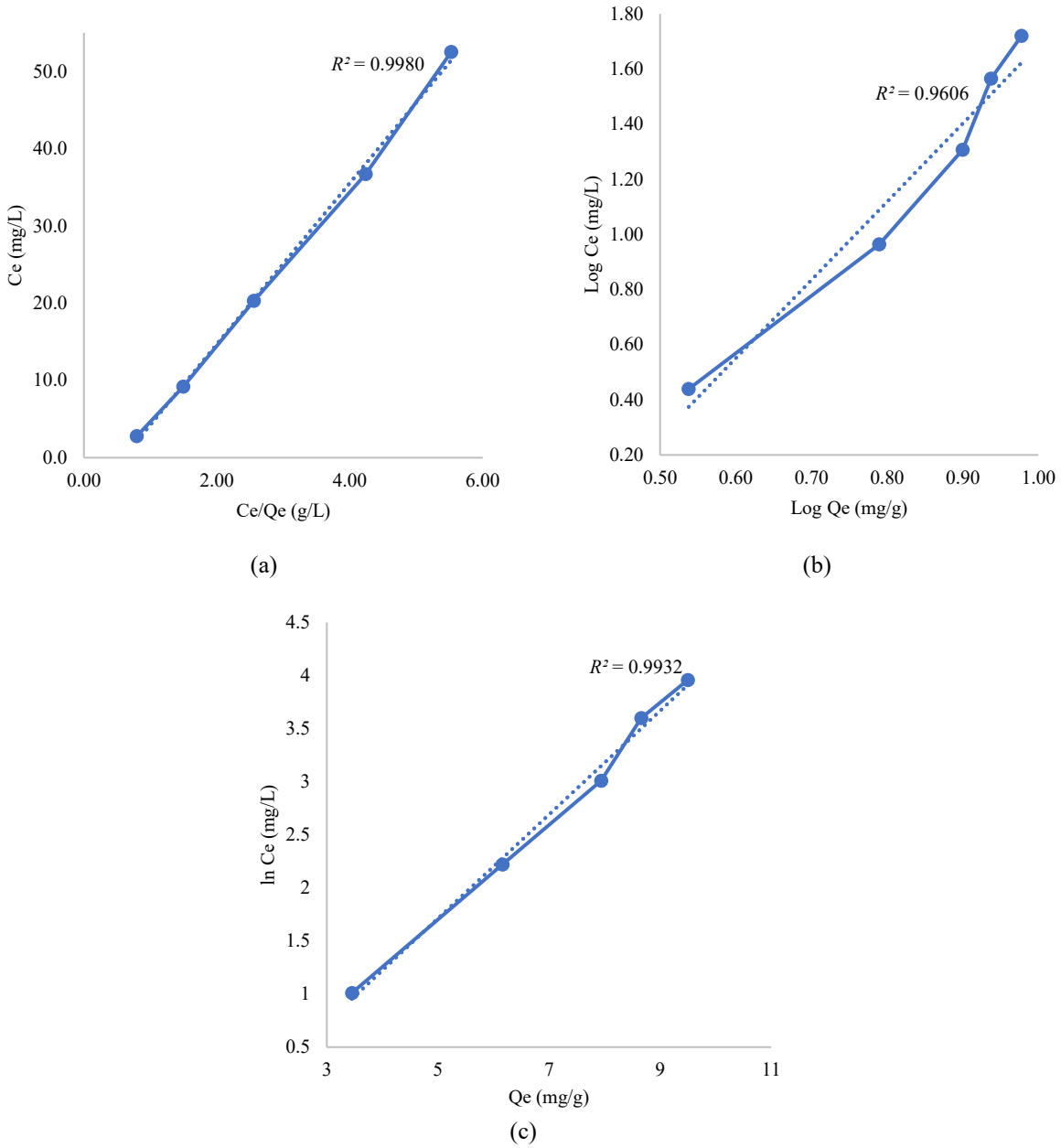

Figure 8. Adsorption isotherm plots for CR adsorption onto CZA: (a) Langmuir isotherm, (b) Freundlich isotherm, and (c) Temkin isotherm

The Freundlich isotherm model, with an R^2 value of 0.9606, also showed a reasonably good fit, suggesting the presence of some surface heterogeneity and adsorption sites with different adsorption energies. However, the higher R^2 value obtained for the Langmuir model indicates that it describes the adsorption behaviour more accurately than the Freundlich model [36]. The Temkin isotherm model, with an R^2 value of 0.9932, indicates that interactions between the dye molecules and the adsorbent also influence the adsorption process [20]. The maximum adsorption capacity (q_{max}) was determined to be 89.29 mg/g, which shows strong adsorption potential [35].

From a practical point of view, these findings mean that CZA can be considered an efficient adsorbent for CR dye removal and that its performance can be reliably predicted using the Langmuir model. Furthermore, Demba et al. [33] reviewed numerous dye adsorption systems and concluded that in most cases equilibrium data fit better to Langmuir, implying dominant monolayer adsorption. This is useful when designing wastewater treatment systems because it

helps estimate how much dye can be removed at different concentrations and how much adsorbent is needed. Overall, the isotherm analysis confirms that CZA has a strong and consistent adsorption capacity for CR dye, and its behaviour follows a predictable monolayer adsorption mechanism [35-37].

3.4. Adsorption Kinetic Analysis

The kinetic analysis provides insight into the rate of CR adsorption by CZA and contributes to understanding the adsorption mechanism. In this study, the equilibrium adsorption capacity was determined to be 3.45 mg/g at 120 min. Based on the linear plots presented in Figure 9(a,b), the pseudo-second-order (PSO) kinetic model provided a better fit to the experimental data than the pseudo-first-order (PFO) model. The PSO model exhibited R^2 of 0.9966, whereas the PFO model showed a considerably lower R^2 value of 0.6408. This strong fit to the PSO model suggests that chemisorption is the main mechanism in this adsorption process rather than just simple physical adsorption [26].

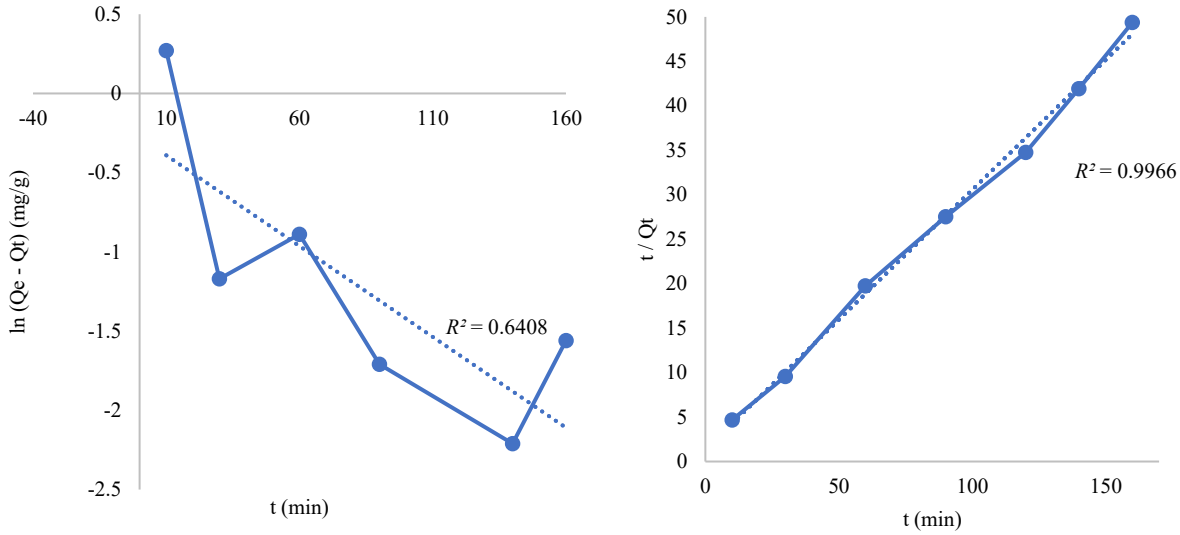

Figure 9. Kinetic plots for CR adsorption onto CZA: (a) PFO and (b) PSO

Similar observations have been reported by Jabar et al. [25], who found that the PSO model best described the adsorption of CR, suggesting that chemisorption was the predominant adsorption mechanism. Likewise, a study on CR adsorption using pine bark reported that the adsorption kinetics were better described by the PSO model ($R^2 > 0.98$) than by the PFO model [31]. These findings indicate that the adsorption kinetics of CR on CZA are consistent with those reported for similar adsorbent systems.

From a practical perspective, the better fit of the PSO model provides useful information for determining the contact time required to achieve optimum dye removal. This information is valuable for the design and optimisation of wastewater treatment systems, enabling efficient operation while minimising processing time and operating costs. Overall, the kinetic analysis demonstrates that CZA is an effective adsorbent for CR removal, with adsorption kinetics that are best described by the PSO model, which is commonly associated with chemisorption.

4. Conclusions

In this study, a successfully synthesised CZA was used to remove CR dye from aqueous solutions. FTIR, XRD, and BET characterisation verified the presence of functional groups, a semi-crystalline structure, and a macroporous surface. Batch adsorption studies showed that pH, contact time, temperature, and adsorbent dosage all had a significant impact on dye removal. A maximum removal efficiency of 98.4% was achieved under the optimum conditions of pH 2, a contact time of 120 min, a temperature of 25°C, an initial dye concentration of 20 mg/L, and an adsorbent dosage of 1.0 g. With a maximum adsorption capacity of 89.29 mg/g, the equilibrium data were best fitted by the Langmuir isotherm model, confirming monolayer adsorption. Kinetic analysis showed that the PSO model provided the best fit for the adsorption process.

Acknowledgement

The authors would like to express their sincere gratitude to Universiti Malaysia Sabah (UMS) for providing the research facilities necessary to conduct this study.

Conflict of interest

The authors declare no conflict of interest.

References

[1] NF Zainudin, ST Sam, YS Wong, H Ismail, S Walli, K Inoue, G Kawamura, WK Tan. Degradation of Diazo Congo red dye by using synthesized poly-ferric-silicate-sulphate through co-polymerization process. Polymers, 2023, 15(1), 237, https://doi.org/10.3390/polym15010237

[2] IH Khalaf, FT Al-Sudani, AA AbdulRazak, T Aldahri, S Rohani. Optimization of Congo red dye adsorption from wastewater by a modified commercial zeolite catalyst using response surface modeling approach. Water Science and Technology, 2021, 83(6*)*, 1369–1383, https://doi.org/10.2166/wst.2021.078

[3] RM Waliullah, AI Rehan, ME Awual, AI. Rasee, MC Sheikh, MS Salman, MS Hossain, MM Hasan, KT Kubra, MN Hasan, HM Marwani, A Islam, MM Rahman, MA Khaleque, MR Awual. Optimization of toxic dye removal from contaminated water using chitosan-grafted novel nanocomposite adsorbent. Journal of Molecular Liquids, 2023, 388, 122763, https://doi.org/10.1016/j.molliq.2023.122763

[4] S Fan, H Guo, Y Wang, J Liu. Selective adsorption of the cationic dye rhodamine-6G from aqueous solution by phosphotungstic acid@MOF-199 composites. Journal of the Indian Chemical Society, 2022, 99(9), 100579, https://doi.org/10.1016/j.jics.2022.100579

[5] BS Damasceno, VC da Silva, AR Rodrigues, EHL Falcão, AC Vaz de Araújo. Use of magnetic nanoparticles of iron oxide and their derivatives in the adsorption of rhodamine 6G and rhodamine B dyes. *Journal of Alloys and Compounds,* 2024, 1005, 175907, https://doi.org/10.1016/j.jallcom.2024.175907

[6] V Katheresan, J Kansedo, SY Lau. Efficiency of various recent wastewater dye removal methods: A review. Journal of Environmental Chemical Engineering, 2018, 6940, 4676–4697, https://doi.org/10.1016/j.jece.2018.06.060

[7] S Jung, M Jung, J Yoon, J Kim, HJ Jin, HW Kwak. Chitosan-derived activated carbon/chitosan composite beads for adsorptive removal of methylene blue and acid orange 7 dyes. Reactive Polymers, 2024, 204, 106028, https://doi.org/10.1016/j.reactfunctpolym.2024.106028

[8] AA Marhoon, SA. Hasbullah, N Asikin-Mijan, WNAW Mokhtar. Adsorption of metal porphyrins using chitosan/zeolite-X composite as an efficient demetallization agent for crude oil: Isotherm, kinetic, and thermodynamic studies. International Journal of Biological Macromolecules, 2024, 274, 133358, https://doi.org/10.1016/j.ijbiomac.2024.133358

[9] NN Safie, AY Zahrim, Recovery of nutrients from sewage using zeolite-chitosan-biochar adsorbent: Current practices and perspectives. Journal of Water Process Engineering, 2021, 40, 101845, https://doi.org/10.1016/j.jwpe.2020.101845

[10] J Kazemi, V Javanbakht. Alginate beads impregnated with magnetic Chitosan@Zeolite nanocomposite for cationic methylene blue dye removal from aqueous solution. International Journal of Biological Macromolecules, 2020, 154, 1426–1437, https://doi.org/10.1016/j.ijbiomac.2019.11.024

[11] GT Şanlı, E Demirhan. Preparation and characterization of chitosan/zeolite composites for Reactive Orange 122 dye removal from aqueous media: isotherm and kinetic studies. Biomass Conversion and Biorefinery, 2024, 15, 3653–3662, https://doi.org/10.1007/s13399-024-05284-z

[12] F Ahmed, T Gulzar, T Kamal, S Kiran, I Ahmad. Phytogenic aqueous extract mediated fabrication of Ag-Fe2O3 nanohybrids for detoxification of carcinogenic Congo Red dye: An Environmental Remediation approach. Global NEST Journal, 2024, 26(7), 1–11, https://doi.org/10.30955/gnj.05516

[13] M. Szymanska-Chargot, A Zdunek. Use of FT-IR Spectra and PCA to the bulk characterization of cell wall residues of fruits and vegetables along a fraction process. Food Biophysics, 2013, 8(1), 29–42, https://doi.org/10.1007/s11483-012-9279-7

[14] A Tahiri, A El-Kordy, Y Elyousfi, L Messaoudi, K Yamni, N Tijani, M Douma, M Messaoudi, L Rghioui. Synthesis of X-type zeolite and their influence on the filtration of dye effluents. Desalination and Water Treatment, 2023, 284, 229–239, https://doi.org/10.5004/dwt.2023.29223

[15] VK Yadav, N Choudhary, D Ali, G Gnanamoorthy, GK Inwati, MHA Almarzoug, G Kumar, SH Khan, MB Solanki. Experimental and computational approaches for the structural study of novel Ca-rich zeolites from incense stick ash and their application for wastewater treatment. Adsorption Science & Technology, 2021, 1–12, https://doi.org/10.1155/2021/6066906

[16] M Harja, N Lupu, H Chiriac, DD Herea, G Buema. Studies on the removal of Congo Red dye by an adsorbent based on fly-Ash@Fe_3O_4 mixture. Magnetochemistry, 2022, 8, 125, https://doi.org/10.3390/magnetochemistry8100125

[17] M Gougazeh, JC Buhl. Synthesis and characterization of zeolite A by hydrothermal transformation of natural Jordanian kaolin. Arab Journal of Basic and Applied Sciences, 2014, 15(1), 35–42, https://doi.org/10.1016/j.jaubas.2013.03.007

[18] TM Budnyak, M Błachnio, A Slabon, A Jaworski, VA Tertykh, A Deryło-Marczewska, AW Marczewski. Chitosan deposited onto fumed silica surface as sustainable hybrid biosorbent for acid orange 8 dye capture: Effect of temperature in adsorption equilibrium and kinetics. Journal of Physical Chemistry C, 2020, 124(28), 15312–15323, https://doi.org/10.1021/acs.jpcc.0c04205

[19] A Kausar, K Naeem, M Tariq, ZIH Nazli, HN Bhatti, F Jubeen, A Nazir, M Iqbal. Preparation and characterization of chitosan/clay composite for direct Rose FRN dye removal from aqueous media: Comparison of linear and non-linear regression methods. Journal of Materials Research and Technology, 2019, 8(1), 1161–1174, https://doi.org/10.1016/j.jmrt.2018.07.020

[20] MA Al-Ghouti, RS Al-Absi. Mechanistic understanding of the adsorption and thermodynamic aspects of cationic methylene blue dye onto cellulosic olive stones biomass from wastewater. Scientific Reports, 2020, 10(1), 1–15, https://doi.org/10.1038/s41598-020-72996-3

[21] SS Ali, R Al-Tohamy, J Sun. Performance of Meyerozyma caribbica as a novel manganese peroxidase-producing yeast inhabiting wood-feeding termite gut symbionts for azo dye decolorization and detoxification. Science of the Total Environment, 2022, 806(3), 150665, https://doi.org/10.1016/j.scitotenv.2021.150665

[22] S Dutta, B Gupta, SK Srivastava, AK Gupta. Recent advances on the removal of dyes from wastewater using various adsorbents: A critical review. Materials Advances, 2021, 2(14), 4497–4531, https://doi.org/10.1039/d1ma00354b

[23] E Rápó, S Tonk. Factors affecting synthetic dye adsorption; desorption studies: A review of results from the last five years (2017–2021). Molecules, 2021, 26, 5419, https://doi.org/10.3390/molecules26175419

[24] S Benkhaya, S M'rabet, A El Harfi. Classifications, properties, recent synthesis and applications of azo dyes. Heliyon, 2020, 6(1), e03271, https://doi.org/10.1016/j.heliyon.2020.e03271

[25] JM Jabar, YA Odusote, KA Alabi, IB Ahmed. Kinetics and mechanisms of Congo-red dye removal from aqueous solution using activated Moringa oleifera seed coat as adsorbent. Applied Water Science, 2020, 10(6), 3–9, https://doi.org/10.1007/s13201-020-01221-3

[26] ED Revellame, DL Fortela, W Sharp, R Hernandez, ME Zappi. Adsorption kinetic modeling using pseudo-first order and pseudo-second order rate laws: A review. Cleaner Engineering and Technology, 2020, 1, 100032, https://doi.org/10.1016/j.clet.2020.100032

[27] VK Gupta, Suhas. Application of low-cost adsorbents for dye removal - A review. Journal of Environmental Management, 2009, 90(8), 2313–2342, https://doi.org/10.1016/j.jenvman.2008.11.017

[28] IO Saheed, NI Zairuddin, SA Nizar, MAKM Hanafiah, AFA Latip, FBM Suah. Adsorption potential of CuO-embedded chitosan bead for the removal of acid blue 25 dye. Ain Shams Engineering Journal, 2024, 15(12), 103125, https://doi.org/10.1016/j.asej.2024.103125

[29] N Jamarun, A Prasejati, Z Zulhadjri, S Caniago, TY Amirullah, W Wulandari, V Sisca. Effect of chitosan concentration on hydroxyapatite/chitosan composite synthesis using the in-situ method as a dye adsorbent. Kuwait Journal of Science, 2024, 51(4), 100252, https://doi.org/10.1016/j.kjs.2024.100252

[30] LP Lingamdinne, GKR Angaru, CA Pal, JR Koduru, RR Karri, NM Mubarak, YY Chang. Insights into kinetics, thermodynamics, and mechanisms of chemically activated sunflower stem biochar for removal of phenol and bisphenol-A from wastewater. Scientific Reports, 2024, 14, 4267, https://doi.org/10.1038/s41598-024-54907-y

[31] ZM Şenol, E Elma, N El Messaoudi, V Mehmeti. Performance of cross-linked chitosan-zeolite composite adsorbent for removal of Pb^{2+} ions from aqueous solutions: Experimental and Monte Carlo simulations studies. Journal of Molecular Liquids, 2023, 391(part A), 123310, https://doi.org/10.1016/j.molliq.2023.123310

[32] M Harja, G Buema, D Bucur. Recent advances in removal of Congo Red dye by adsorption using an industrial waste. Scientific Reports, 2022, 12(1), 1–15, https://doi.org/10.1038/s41598-022-10093-3

[33] AD N'diaye. Modeling of adsorption isotherms of dyes onto various adsorbents: A short review. Arabian Journal of Chemical and Environmental Research, 2018, 5, 42–51.

[34] S Samsami, M Mohamadi, MH Sarrafzadeh, ER Rene, M Firoozbahr. Recent advances in the treatment of dye-containing wastewater from textile industries: Overview and perspectives. Process Safety and Environmental Protection, 2020, 143, 138–163, https://doi.org/10.1016/j.psep.2020.05.034

[35] MA Farghali, AM Selim, HF Khater, N Bagato, W Alharbi, KH Alharbi, TI Radwan. Optimized adsorption and effective disposal of Congo red dye from wastewater: Hydrothermal fabrication of MgAl-LDH nanohydrotalcite-like materials. Arabian Journal of Chemistry, 2022, 15(96), 104171, https://doi.org/10.1016/j.arabjc.2022.104171

[36] K Duodu, GW Ashong, TR Agbetsi, J Wuloh, A Kangmennaa, CO Agyapong, NO Boadi, ES Agorku. Congo red adsorption in water using a novel nano zero-valent iron intercalated Zn–Al–CO3 layered double hydroxide: adsorption isotherm, kinetics and thermodynamics. Discover Applied Sciences, 2025, 7(6), 606, https://doi.org/10.1007/s42452-025-06616-y

[37] K Litefti, MS Freire, M Stitou, J González-Álvarez. Adsorption of an anionic dye (Congo red) from aqueous solutions by pine bark. Scientific Reports, 2019, 9, 16530, https://doi.org/10.1038/s41598-019-53046-z